TU Delft

Delft University of Technology

Projection lens testing with Moiré effect

Loktev, M.; Shao, Y.

DOI
10.1117/12.2264343

Publication date
2017

Document Version
Final published version

Published in
Metrology, Inspection, and Process Control for Microlithography XXXI

Citation (APA)
Loktev, M., & Shao, Y. (2017). Projection lens testing with Moiré effect. In M. I. Sanchez (Ed.), *Metrology, Inspection, and Process Control for Microlithography XXXI* [101452S] (Proceedings of SPIE; Vol. 10145). SPIE. https://doi.org/10.1117/12.2264343

Important note
To cite this publication, please use the final published version (if applicable).
Please check the document version above.

Copyright
Other than for strictly personal use, it is not permitted to download, forward or distribute the text or part of it, without the consent of the author(s) and/or copyright holder(s), unless the work is under an open content license such as Creative Commons.

Takedown policy
Please contact us and provide details if you believe this document breaches copyrights.
We will remove access to the work immediately and investigate your claim.

This work is downloaded from Delft University of Technology.
For technical reasons the number of authors shown on this cover page is limited to a maximum of 10.

PROCEEDINGS OF SPIE

SPIEDigitalLibrary.org/conference-proceedings-of-spie

Projection lens testing with Moiré effect

M. Loktev, Y. Shao

M. Loktev, Y. Shao, "Projection lens testing with Moiré effect," Proc. SPIE 10145, Metrology, Inspection, and Process Control for Microlithography XXXI, 101452S (28 March 2017); doi: 10.1117/12.2264343

SPIE.

Event: SPIE Advanced Lithography, 2017, San Jose, California, United States

Downloaded From: https://www.spiedigitallibrary.org/conference-proceedings-of-spie on 2/26/2018 Terms of Use: https://www.spiedigitallibrary.org/terms-of-use

Projection lens testing with Moiré effect

M. Loktev*[a], Y. Shao[b]
[a]Liteq BV, Esp 314, 5633AE Eindhoven, the Netherlands
[b]Delft University of Technology, Faculty of Applied Sciences,
Optics Research Group, Van der Waalsweg 8, 2628CH Delft, the Netherlands
*E-mail: mikhail.loktev@liteq.nl

ABSTRACT

The application of Moiré effect for testing of a lithographic projection lens is reported. The arrangement presented allows measuring magnification, distortion, field curvature and telecentricity of the lens and can be used for its fine tuning. The method is based on two matched two-dimensional gratings, positioned in mutually conjugated planes; one of them can be translated. Visual interpretation of Moiré fringe pattern allows quick diagnostics of position errors exceeding critical dimension, whereas lateral scanning is applied for measuring of smaller magnitude errors. Field curvature and telecentricity are measured by 3D scanning. Presented results are in a good agreement with those obtained elsewhere.

Keywords: lithography, projection lens, optical metrology, distortion, Moiré effect

1. INTRODUCTION

Distortion of the projection optics is critical for overlay performance of a lithographic projection tool. Typical distortion spec is an order of magnitude smaller than critical dimension (CD) of the projection tool. To achieve the final spec, the manufacturer of the projection lens should be able to measure distortion with sufficient accuracy (typically, order of magnitude finer) to provide feedback for fine-tuning the lens. Even for non-critical lithography tools with CD in a micron range, it means ~100 nm distortion measured with ~10 nm accuracy. This is a challenging task for an optical manufacturer. It requires building a dedicated measurement tool, which is comparable in complexity with fully functional lithographic system and requires thermally stable vibration-free environment.

The use of Moiré effect for distortion measurement is reported since 1980s [1,2]. The basic idea is quite simple. It is based on analysis of low-frequency fringe pattern obtained by superposition of two identical gratings. If the first grating is projected through the lens, and its aerial image is superimposed with the second grating, then fringe analysis allows reconstructing distortion of the lens. Variations of this idea resulted in several measurement schemes patented by IBM, Nikon and Zeiss [1,3,4].

Besides distortion, projection lenses should be characterized for other wavefront aberrations in the whole field. Interferometric testing requires measurement point by point, which is rather time-consuming and susceptible to drifts and vibrations. In case the lens is fine tuned for distortion, special care should be taken to keep other aberrations under control while correcting distortion. A setup that measures distortion and wavefront aberrations at the same time would significantly reduce effort on optimization and characterization of the optics.

In this paper, we present results of testing of a lithographic projection stepper lens in an optical scheme based on Moiré effect. As demonstrated experimentally, the arrangement presented allows measuring magnification, distortion, field curvature and telecentricity of the lens and can be used for its fine tuning. The method is based on two matched two-dimensional gratings (arrays of pinholes) whose feature size is comparable with critical dimension of the projection system and whose position errors are two orders of magnitude smaller. The first grating is positioned before the lens (in the “object” plane) and illuminated with a Köhler illumination system. The second grating is placed in a conjugated (“image”) plane and can be translated both laterally (in X and Y) and axially (in Z).

In the presented theoretical analysis of the Moiré fringe forming, local intensity after the second mask is considered as a periodic function of lateral shift between the gratings. Variation of the transmission profile and its contrast due to diffraction effects, aberrations and defocus is analyzed.

Visual interpretation of Moiré fringe pattern allows quick diagnostics of placement errors of the projection system (i.e., combined distortion and magnification error). If placement errors exceed the critical dimension and the masks are

Metrology, Inspection, and Process Control for Microlithography XXXI, edited by Martha I. Sanchez, Vladimir A. Ukraintsev
Proc. of SPIE Vol. 10145, 101452S · © 2017 SPIE · CCC code: 0277-786X/17/$18 · doi: 10.1117/12.2264343

Downloaded From: https://www.spiedigitallibrary.org/conference-proceedings-of-spie on 2/26/2018 Terms of Use: https://www.spiedigitallibrary.org/terms-of-use

aligned by rotation, one could tell the magnitude of these errors from the number of fringes and, based on their shape, relative contributions of magnification and distortion.
Lateral scanning schemes can be applied for measuring of smaller magnitude errors with accuracy up to a few tens of nm. One approach is similar to the phase shifting method in interferometry, where the mask is translated in a few steps and local position error is extracted from the phase of periodic intensity variation. Another approach treats the second mask as a sampling tool for simultaneous scanning of the PSFs at different positions in the field-of-view generated by the corresponding pinholes in the first mask. In this case, placement error manifests itself as a PSF shift. We found that both reconstruction methods lead to similar results. Further, we analyzed measurement errors caused by aberrations and defocus and found that certain asymmetric aberrations (such as coma) may influence the reconstruction result, which should be considered for high precision measurements.

2. APPROACH

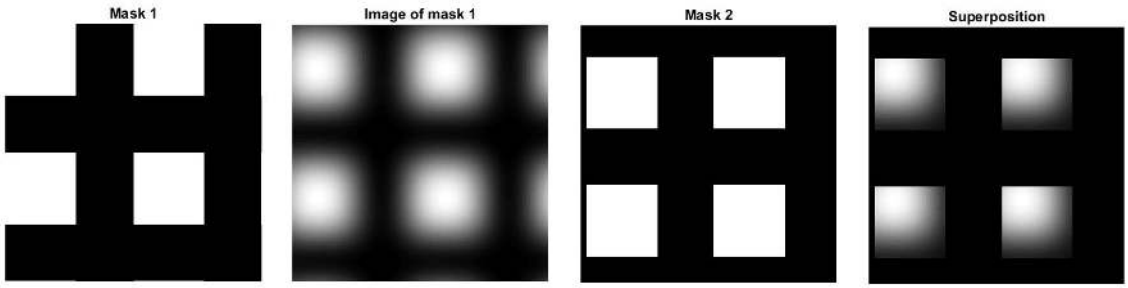

Figure 1. Mask 1 imaged through the system and superimposed into mask 2; simulation.

Let us consider two identical linear gratings with a few microns' period, whose pattern can only be resolved under a microscope. If these gratings are superimposed, a macroscopic-scale Moiré fringe pattern can be seen in transmission. If the lines of both gratings are perfectly aligned by rotation, the pattern will be simplified to a single fringe with uniform transmission, which is insensitive to relative shift between the gratings in direction parallel to the lines and highly sensitive to shift in perpendicular direction. In the latter case, submicron shifts can be detected by monitoring change in transmission. Maximum transmission corresponds to whole-period shifts of ±nT, where n is an integer number and T is the grating period, whereas minimum transmission corresponds to half-period shifts of ±(n+1/2)T. A similar arrangement sensitive to shifts in both directions can be made using gratings with two-dimensional structure, such as orthogonal grid of pinholes.

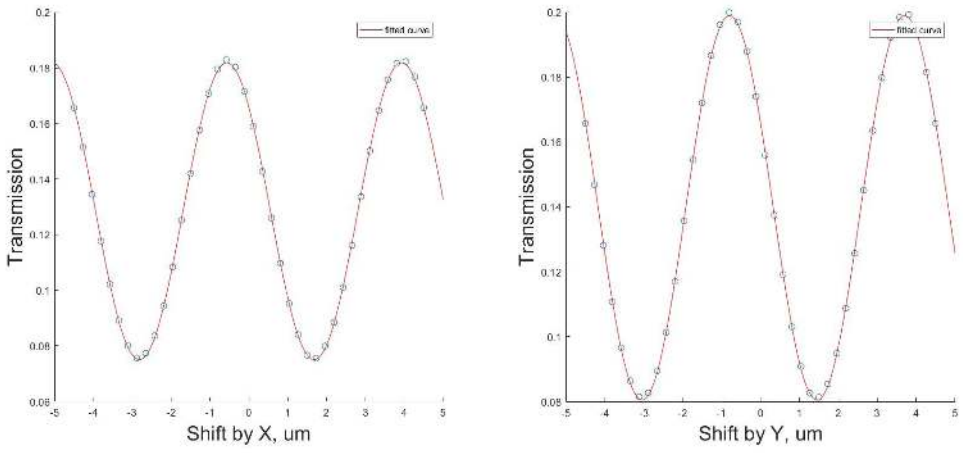

Figure 2. Simulated local transmission vs lateral shift, X and Y scans.

Downloaded From: https://www.spiedigitallibrary.org/conference-proceedings-of-spie on 2/26/2018 Terms of Use: https://www.spiedigitallibrary.org/terms-of-use

Let us consider two masks consisting of matching two-dimensional pinhole patterns (see Figure 1). Mask 1 is situated in the "object" plane of a projection system and is projected through the lens to the "image" plane, where the image is superimposed on mask 2. In case the feature size is comparable with critical dimension of the projection system, the image is slightly blurred; besides, the pattern is subjected to local shifts caused by the lens distortion. Superposition with mask 2 cuts off part of the blurred image, which is seen on the macro scale as local transmission change.
If one of the gratings is laterally translated in X or Y, one can observe periodic change in local transmission, which is close to sinusoidal one (see Figure 2). By locating the maximum of the transmission curve, one can find X and Y translations which correct for shift between the patterns. Processing a set of full-field transmission patterns corresponding to a series of lateral mask translations, one can reconstruct the distortion pattern.
More information can be extracted by applying a 3D scanning sequence.

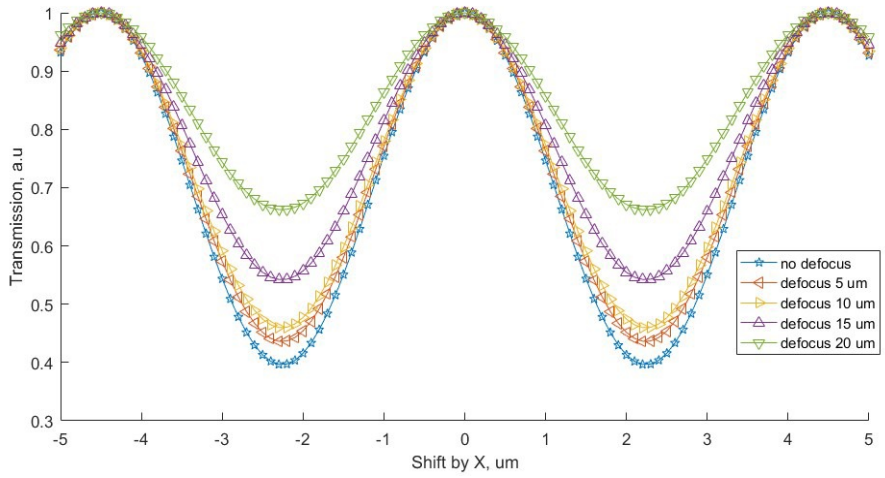

(a)

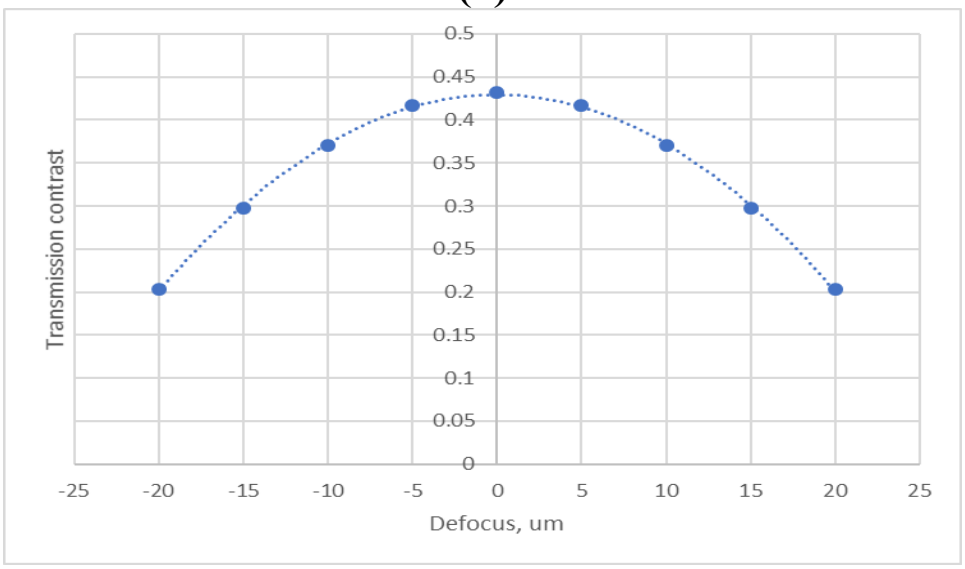

(b)

Figure 3. Simulated local transmission vs lateral shift vs defocus between the masks (a); transmission contrast vs defocus.

Downloaded From: https://www.spiedigitallibrary.org/conference-proceedings-of-spie on 2/26/2018 Terms of Use: https://www.spiedigitallibrary.org/terms-of-use

1) **Object side telecentricity.** It requires two distortion measurements with a small axial (Z) shift of mask 1 between the measurements. The telecentricity pattern is calculated as a difference of measured distortion patterns divided by Z shift.
2) **Image side telecentricity.** The scheme is similar to the previous one, but mask 2 is shifted instead of mask 1.
3) **Field curvature.** As shown in Figure 3a, defocus between the masks reduces the contrast of local transmission curve. In this example, defocus is introduced by axial shift of mask 2. Making lateral scans at different positions in Z and plotting contrast vs Z as shown in Figure 3b, one can detect the best focus by finding the maximum. Performing this reconstruction for several field points, one can find the variation of best focus vs field, i.e., which can be interpreted as field curvature. Due to astigmatism, scanning in X and Y results in different results for best focus. To estimate field curvature, we will take the average of these values.
4) **Astigmatic difference** is the difference in best focus between vertical and horizontal features caused by astigmatism. The measurement scheme is the same as for field curvature; the astigmatic difference is calculated as a difference of best focus values obtained from X and Y scans.

3. SIMULATION

We built a model which simulates transmission of superimposed masks, considering wavefront aberrations of the projection system and defocus between the masks. In our analysis, we have considered measuring 1x magnification lens with numerical aperture NA=0.128, operating at 355 nm wavelength, which has critical dimension <2 μm and 52 mm x 33 mm field. For Moiré test we used a pinhole grating mask configuration with 4.5 μm x 4.5 μm period. To improve sensitivity of the test, we made the pinhole slightly larger than half period of the mask, 2.5 μm x 2.5 μm. To characterize the accuracy of Moiré method for distortion measurement in aberrated lenses, we have compared value of distortion measured by shift of the transmission curve in Moiré test with those calculated from PSF centroid. Table 1 shows the maximum difference based on X and Y scans. Scanning was centered at three different positions with (0, 0), (1mm, 1mm) and (2.5 mm, 2.5 mm) shift between masks. The accuracy of the simulation was limited to ~10 nm due to image discretization.

Table 1. Simulated difference of distortion measured in Moiré test and distortion calculated from PSF centroid, in nm.

Scanning position	(0, 0)	(1 mm, 1 mm)	(2.5 mm, 2.5 mm)
No aberrations, in focus	9.7	10.2	10.4
No aberrations, defocus 5 μm	9.9	10.4	10.6
No aberrations, defocus 10 μm	10.3	11.0	11.5
Z5 = 0.1 λ, in focus	9.9	10.4	10.4
Z5 = 0.1 λ, defocus 5 μm	10.4	10.9	11.1
Z5 = 0.1 λ, defocus 10 μm	11.4	12.0	12.9
Z7 = 0.1 λ, in focus	46.2	37.3	10.6
Z7 = 0.1 λ, defocus 5 μm	57.1	49.0	16.1
Z7 = 0.1 λ, defocus 10 μm	93.0	87.8	63.9
RMS WFE = 0.015 λ, in focus	9.2	7.9	16.4
RMS WFE = 0.015 λ, defocus 5 μm	10.2	2.5	16.1
RMS WFE = 0.015 λ, defocus 10 μm	13.7	7.7	18.1
RMS WFE = 0.035 λ, in focus	15.0	15.2	3.3
RMS WFE = 0.035 λ, defocus 5 μm	19.3	32.8	7.7
RMS WFE = 0.035 λ, defocus 10 μm	32.3	63.2	17.8

As seen in Table 1, the measurement error is insignificant and shows little variation with focus in the following cases:

- absence of aberrations,
- random combination of Zernike aberrations with low magnitude (RMS wavefront error 0.015 λ), and
- pure astigmatism (Z5 = 0.1 λ).

Downloaded From: https://www.spiedigitallibrary.org/conference-proceedings-of-spie on 2/26/2018 Terms of Use: https://www.spiedigitallibrary.org/terms-of-use

However, the presence of coma (term Z7 = 0.1 λ of Zernike fringe polynomials) has significant influence on the measurement error, which is related to asymmetry of the PSF caused by this aberration. Asymmetric aberrations also play a role in a situation when random aberrations have larger magnitude (RMS wavefront error 0.035 λ); here we can see the measurement error growing with defocus. For high precision measurements, defocus in the optical scheme should be minimized, and the influence of coma should be considered.

4. EXPERIMENT

The method described in section 2 was applied to testing of the first prototype of 1x projection lens developed by Liteq. Some of the test results are included in this section; these do not represent the performance of the final lens design.
To understand how a Moiré fringe pattern is formed, we should consider three different sorts of position errors.

1) **Rotation between the masks** creates a regular pattern with structure which matches the mask geometry; in our case, a rectangular pattern. The number of fringes over the field increases with rotation angle; it can be estimated as $N=\alpha \cdot D/T$, where α is the rotation angle, D is the field size and T is the mask period. It can be minimized by fine adjusting rotation of one of the masks.
2) **Lens magnification** creates a regular fringe pattern like those resulting from rotation; an example is shown in Figure 4(c). The number of fringes can be estimated as $N=M \cdot D/T$, where M is the magnification factor. In case when magnification is combined with rotation, fringes appear tilted with respect to the mask pattern, as shown in Figure 4(b).
3) **Lens distortion** creates an irregular fringe pattern which is easier to interpret in the presence of rotation or magnification (see Figure 4(a)). In this case, deformation of the regular fringe pattern counted in fringes can be used to estimate the magnitude of distortion: $|Distortion| \approx N \cdot T$, where N is the number of fringes of deformation.

Figure 4 shows the results of four steps in optimization of the measurement scheme. As seen in Figure 4(a), we started from distortion exceeding 9 μm, which is >2 fringes of deformation. By optimization of the conjugate planes, we have

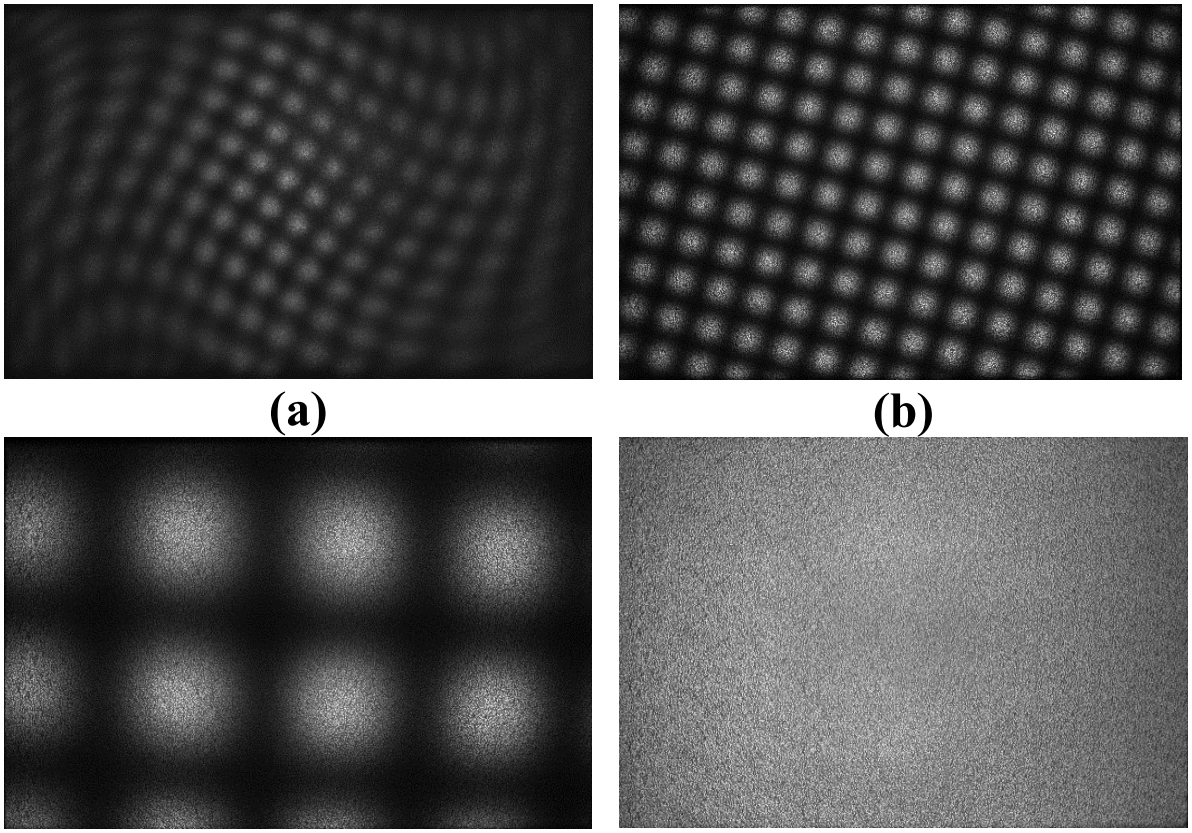

Figure 4. Moiré fringe patterns resulting from large distortion, rotation and magnification (a), small distortion, rotation and magnification (b), small distortion and magnification (c), and small distortion only (d).

Downloaded From: https://www.spiedigitallibrary.org/conference-proceedings-of-spie on 2/26/2018 Terms of Use: https://www.spiedigitallibrary.org/terms-of-use

managed to reduce it to the level of <0.5 μm when it became difficult to distinguish by fringes (Figure 4(b)). Correcting tilt in the fringe pattern by mask rotation adjustment, we have obtained pattern Figure 4(c) which shows magnification error ~9 μm (2 fringes) per half field. After correcting it using zoom control of the projection lens, we have obtained virtually uniform transmission over the field (Figure 4(d)), where no fringes can be distinguished.

At this point, scanning can be applied for measurement of the remaining distortion, rotation and magnification. We have measured two configurations of the projection lens (further referred to as "Zoom 1" and "Zoom 2"), only different by zoom settings. Raw Moiré patterns for Zoom 1 and Zoom 2 configurations can be seen in Figure 4(c) and 4(d), and the reconstruction results are presented in Figures 5 and 6. Rotation and magnification were extracted in post-processing. As shown in Figure 5(a), combined magnification and distortion of Zoom 1 configuration amounts to 9182 nm, which is close to 9 um estimate based on number of fringes. Figure 6(a) shows that, in case of Zoom 2, the magnification is largely corrected. Extracting magnification results in very similar patterns for Zoom 1 and Zoom 2 (Figures 5(b) and 6(b)), which agrees with the fact that our concept of zoom adjustment has marginal effect on distortion.
Further, we have applied scanning in 3D to measure telecentricity and field curvature of the test system. As seen in Figure 7, the measured telecentricity pattern is in good agreement with those simulated in a ray tracing model. The field curvature pattern measured in a Moire test (see Figure 8) show good matching with those obtained interferometrically.

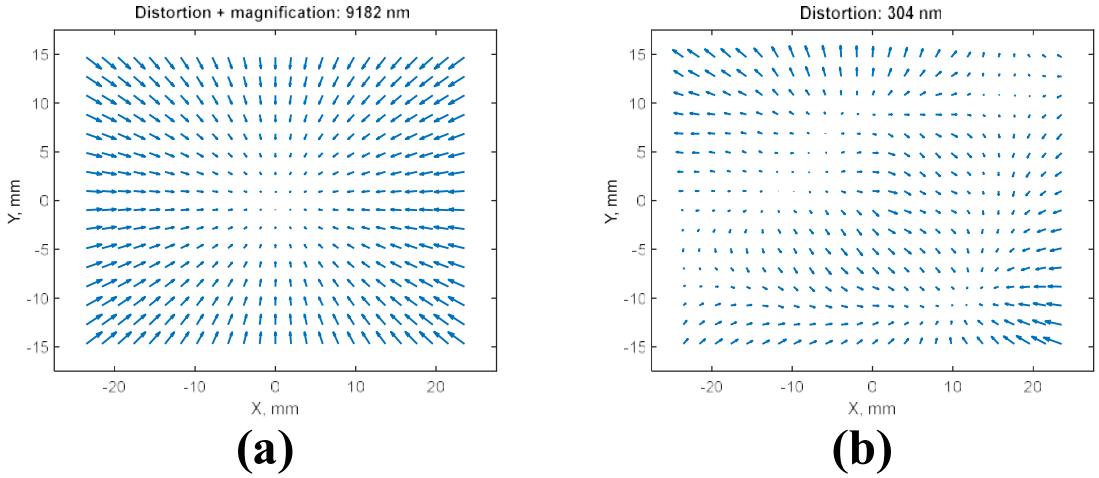

Figure 5. Distortion + magnification (a) and pure distortion (b) in Zoom 1 configuration, measured in a scanning test.

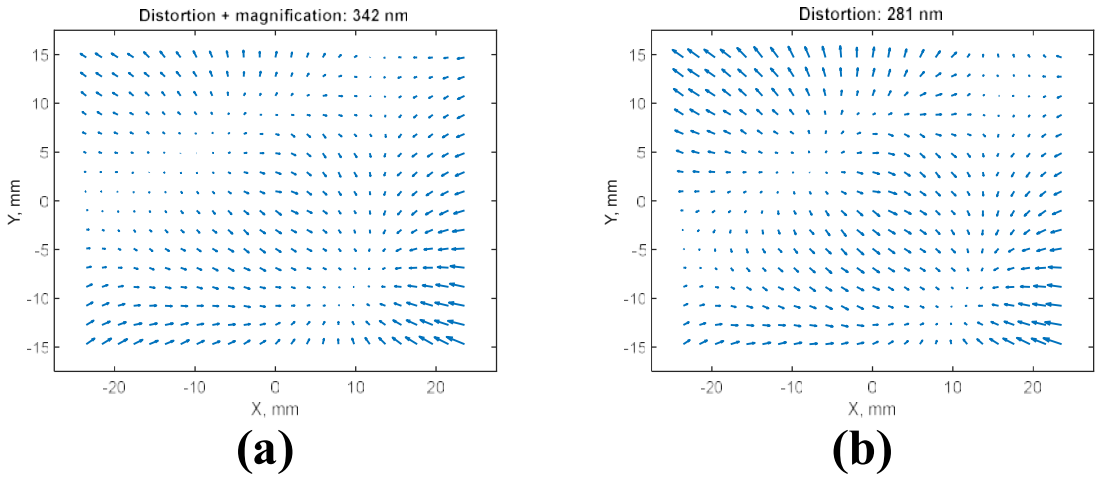

Figure 6. Distortion + magnification (a) and pure distortion (b) in Zoom 2 configuration, measured in a scanning test.

Downloaded From: https://www.spiedigitallibrary.org/conference-proceedings-of-spie on 2/26/2018 Terms of Use: https://www.spiedigitallibrary.org/terms-of-use

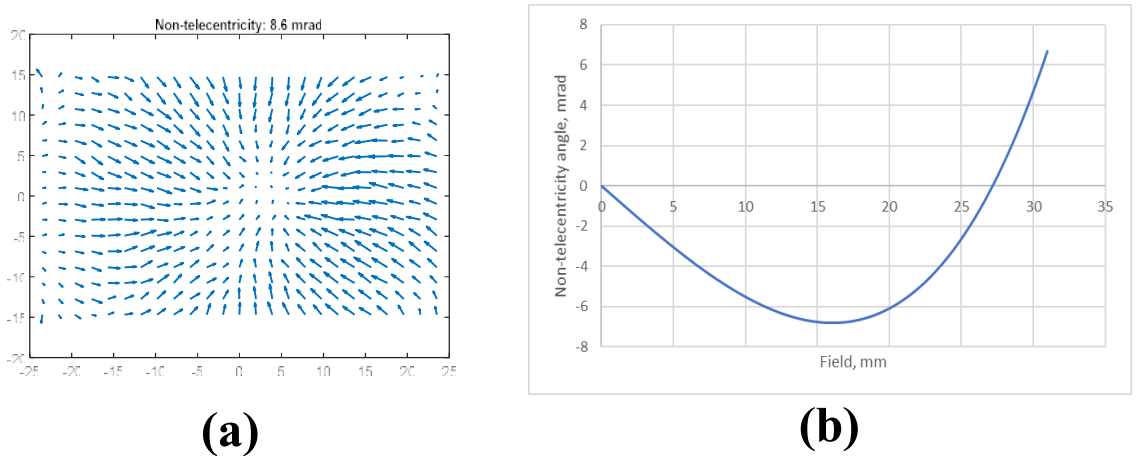

Figure 7. Combined non-telecentricity of the test system (illumination + projection optics), as measured by 3D scanning (a) and simulated in a ray tracing model (b).

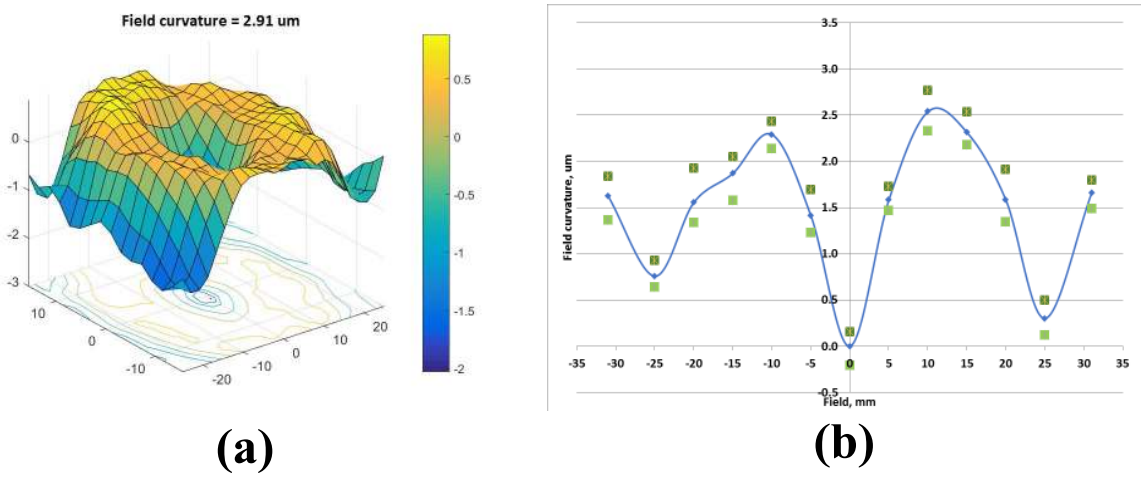

Figure 8. Field curvature measured by 3D scanning (a) and in an interferometric test (b).

5. CONCLUSION

As shown in this paper, optical test based on Moiré effect can be made highly flexible by combining it with 2D and 3D scanning. It can be applied for measuring different characteristics of a projection lens, such as magnification, distortion, field curvature and telecentricity. Both quick diagnostics of the distortion by visual fringe analysis and high-precision scanning measurement can be used for optimization of the imaging scheme, minimizing its magnification and distortion.

Downloaded From: https://www.spiedigitallibrary.org/conference-proceedings-of-spie on 2/26/2018 Terms of Use: https://www.spiedigitallibrary.org/terms-of-use

REFERENCES

[1] Haeusler, G. and Jaerisch, W., "Method of Moiré-metrical testing of optical imaging systems", U.S. Patent 4,386,849 (1983).

[2] Chang, R.-S. and Lee, C.-C., "The measurement of aberration by Moiré pattern", Proc. SPIE, 649 (1990).

[3] Kobayashi, N., "Lens distortion measurement using Moiré fringes", U. S. Patent 5,973,773 (1999).

[4] Heppner, J., Massig, J., Arnz, M., Kuechel, M., Penzing, J., and Schellhorn, U., "Moiré method and a system for measuring the distortion of an optical imaging system", U.S. Patent 6,816,247 B1 (2004).

[5] Wegmann, U., Schellhorn, U., Klaesges, R. and Stuehler, J., "Moiré method and measuring system for measuring the distortion of an optical imaging system", U.S. Patent 7,019,824 B2 (2006).

Downloaded From: https://www.spiedigitallibrary.org/conference-proceedings-of-spie on 2/26/2018 Terms of Use: https://www.spiedigitallibrary.org/terms-of-use